Journal of Geophysical Research: Atmospheres

RESEARCH ARTICLE
10.1029/2018JD028759

Estimating Regional Ground-Level $PM_{2.5}$ Directly From Satellite Top-Of-Atmosphere Reflectance Using Deep Belief Networks

Huanfeng Shen[1,2,3], Tongwen Li[1], Qiangqiang Yuan[2,4], and Liangpei Zhang[2,5]

[1]School of Resource and Environmental Sciences, Wuhan University, Wuhan, China, [2]The Collaborative Innovation Center for Geospatial Technology, Wuhan, China, [3]The Key Laboratory of Geographic Information System, Ministry of Education, Wuhan University, Wuhan, China, [4]School of Geodesy and Geomatics, Wuhan University, Wuhan, China, [5]The State Key Laboratory of Information Engineering in Surveying, Mapping and Remote Sensing, Wuhan University, Wuhan, China

Key Points:
- We estimated ground-level $PM_{2.5}$ directly from satellite TOA reflectance rather than satellite AOD
- The deep learning based model achieved a state-of-the-art performance in the estimation of ground $PM_{2.5}$ over Wuhan Urban Agglomeration
- The TOA-reflectance-derived $PM_{2.5}$ has a finer resolution and a larger spatial coverage than the AOD-derived $PM_{2.5}$

Supporting Information:
- Supporting Information S1

Correspondence to:
Q. Yuan,
yqiang86@gmail.com

Citation:
Shen, H., Li, T., Yuan, Q., & Zhang, L. (2018). Estimating regional ground-level $PM_{2.5}$ directly from satellite top-of-atmosphere reflectance using deep belief networks. *Journal of Geophysical Research: Atmospheres*, *123*, 13,875–13,886. https://doi.org/10.1029/2018JD028759

Received 3 APR 2018
Accepted 27 NOV 2018
Accepted article online 7 DEC 2018
Published online 21 DEC 2018

Abstract Almost all remote sensing atmospheric $PM_{2.5}$ estimation methods need satellite aerosol optical depth (AOD) products, which are often retrieved from top-of-atmosphere (TOA) reflectance via an atmospheric radiative transfer model. Then, is it possible to estimate ground-level $PM_{2.5}$ directly from satellite TOA reflectance without a physical model? In this study, this challenging work was achieved based on a machine learning model. Specifically, we established the relationship between $PM_{2.5}$, satellite TOA reflectance, observation angles, and meteorological factors in a deep learning architecture (denoted as Ref-PM modeling). This relationship was trained with station $PM_{2.5}$ measurements, and then the $PM_{2.5}$ values of those locations without stations could be retrieved. Taking the Wuhan Urban Agglomeration as a case study, the results demonstrate that, compared with AOD-PM modeling, the Ref-PM modeling obtains a competitive performance, with sample-based cross-validated R^2 and root-mean-square error values of 0.87 and 9.89 $\mu g/m^3$, respectively. Also, the TOA-reflectance-derived $PM_{2.5}$ has a finer resolution and a larger spatial coverage than the AOD-derived $PM_{2.5}$. This work provides an alternative technique to estimate ground-level $PM_{2.5}$, and may have the potential to promote the application in atmospheric environmental monitoring.

1. Introduction

Fine particulate matter ($PM_{2.5}$, airborne particles of less than 2.5 μm in aerodynamic diameter) has been reported to be associated with many health problems, including cardiovascular and respiratory morbidity and mortality (Habre et al., 2014; Madrigano et al., 2013). Previous studies have indicated that severe $PM_{2.5}$ pollution resulted in more than 3 million premature deaths around the world in 2010 (Lim et al., 2012). There is thus an urgent need to acquire accurate spatiotemporal distributions of ground-level $PM_{2.5}$ concentrations for the environmental health concerns (Brauer et al., 2012; Crouse et al., 2012).

The satellite-derived aerosol optical depth (AOD) products have been extensively employed to expand $PM_{2.5}$ estimation beyond that only provided by ground monitoring stations (Hoff & Christopher, 2009; Lary et al., 2014, 2015; Z. Li et al., 2016). The AOD products used include those retrieved from the Moderate Resolution Imaging Spectroradiometer (MODIS; Fang et al., 2016), the Multiangle Imaging Spectroradiometer (You et al., 2015), the Visible Infrared Imaging Radiometer Suite (Wu et al., 2016), and the Geostationary Operational Environmental Satellite Aerosol/Smoke Product (Paciorek et al., 2008), and so forth. In addition, many different models have been developed to establish the relationship between AOD and $PM_{2.5}$ (denoted as AOD-PM modeling), such as multiple linear regression (Gupta & Christopher, 2009b), geographically weighted regression (Hu et al., 2013), linear mixed effects model (Lee et al., 2011a), neural networks (Gupta & Christopher, 2009a; T. Li, Shen, Zeng et al., 2017), and so on. Based on these models, satellite-derived AOD products have played an important role in the estimation of ground-level $PM_{2.5}$ (Lee et al., 2011b; Liu et al., 2009; Martin, 2008; van Donkelaar et al., 2016).

The AOD products are often retrieved from satellite top-of-atmosphere (TOA) reflectance through an atmospheric radiative transfer model (e.g., second simulation of the satellite signal in the solar spectrum [6S], MODerate resolution atmospheric TRANsmission [MODTRAN]; Hsu et al., 2004; Kaufman, Tanré et al., 1997; Levy et al., 2007). Hence, the previous procedure of satellite-based $PM_{2.5}$ estimation usually involves two steps. The first step is to retrieve the AOD from the satellite TOA reflectance, this process may not be necessary for researchers focusing on $PM_{2.5}$ estimation (e.g., MODIS AOD can be obtained from the NASA website). The second step is to estimate the ground-level $PM_{2.5}$ from the satellite-derived AOD. A challenging

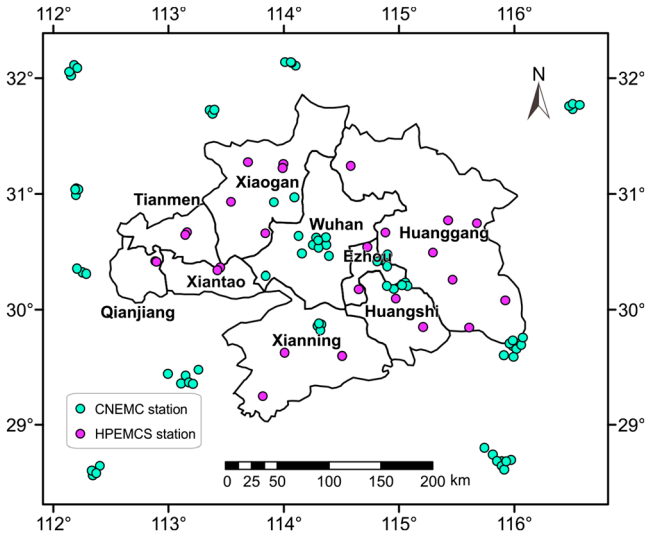

Figure 1. Study region and the spatial distribution of $PM_{2.5}$ stations. CNEMC = China National Environmental Monitoring Center; HPEMCS = Hubei Provincial Environmental Monitoring Center Station.

proposition is whether it is possible to avoid the intermediate process of AOD retrieval and to estimate ground-level $PM_{2.5}$ directly from satellite TOA reflectance (denoted as Ref-PM modeling). Actually, previous studies have provided some potentials for Ref-PM modeling. On the one hand, some researchers (Radosavljevic et al., 2007; Ristovski et al., 2012) have adopted neural networks to learn a functional relationship between MODIS observations and ground-observed AOD, and neural network-based AOD retrieval has achieved satisfactory results when compared with the physically retrieved AOD. On the other hand, many aforementioned models have been employed to establish the AOD-$PM_{2.5}$ relationship. Given that the physical retrieval of AOD from TOA reflectance can be simulated using statistical approaches, as well as the AOD-$PM_{2.5}$ relationship, it appears possible to directly model the statistical relationship between TOA reflectance and ground-level $PM_{2.5}$.

Anyhow, it would be very complicated to estimate ground-level $PM_{2.5}$ from satellite TOA reflectance in one step. The retrieval of AOD from satellite TOA reflectance is a nonlinear physical problem; the satellite-derived AOD in conjunction with auxiliary factors (e.g., meteorological parameters) is also usually nonlinearly correlated with $PM_{2.5}$ (Zheng et al., 2017). Hence, the estimation of ground-level $PM_{2.5}$ directly from TOA reflectance is highly complex, and the conventional models may encounter some challenges. Deep learning, which is a further development of neural networks, has been used for time series prediction (Ong et al., 2015) and satellite AOD-based estimation (T. Li, Shen, Yuan et al., 2017) of ground-level $PM_{2.5}$. The deep learning models have shown the ability to effectively predict/estimate ground-level $PM_{2.5}$, which can be attributed to their ability to fit nonlinear and complicated relationships (Hinton et al., 2006; LeCun et al., 2015). Thus, deep learning may be a good tool for satellite TOA reflectance based estimation of ground-level $PM_{2.5}$.

The objective of this study is to develop a deep learning-based modeling for the estimation of ground-level $PM_{2.5}$ using satellite TOA reflectance rather than satellite AOD products. To be specific, a deep belief network (DBN; Hinton et al., 2006) model will be employed to establish the relationship between ground-level $PM_{2.5}$, satellite TOA reflectance, observation angles, and meteorological factors. Through the Ref-PM modeling, we can not only simplify the procedure of satellite-based $PM_{2.5}$ estimation, but also avert the accumulative error of AOD retrieval (Munchak et al., 2013). The proposed Ref-PM modeling will be validated with data from the Wuhan Urban Agglomeration (WUA; Figure 1) covering the whole year of 2016.

2. Study Region and Data

2.1. Study Region

The study region was the WUA, which is presented in Figure 1. The study period was the whole year of 2016. The WUA is located in Hubei province, central China. To make full use of the $PM_{2.5}$ station measurements, all the monitoring stations in the latitude range of 28.4°–32.3°N and longitude range of 112.0°–116.7°E were included in our analysis. The WUA is a city group made up of the city of Wuhan and eight adjacent cities (Huangshi, Ezhou, Huanggang, Xiaogan, Xianning, Xiantao, Qianjiang, and Tianmen). It has a total population of more than 30 million, which accounts for more than half of the total population of Hubei province. With over 60% of the gross domestic product of Hubei province, the WUA is one of the largest urban groups in central China (Tan et al., 2014). In 2007, the WUA was designated as one of the pilot areas for "national resource-saving and environment-friendly society" by the Chinese government.

Due to the dense urbanization and industrial activities, the WUA has been suffering serious air pollution. Previous studies have reported that Wuhan is especially affected by fine-mode particles (Wang et al., 2014, 2015). Moreover, with the rapid economic development, the other cities in the WUA (e.g., Ezhou and Huangshi) also have high levels of $PM_{2.5}$ concentration. It is thus urgent and necessary to obtain the spatiotemporal distribution of $PM_{2.5}$ in this area.

2.2. Ground-Level $PM_{2.5}$ Measurements

Hourly $PM_{2.5}$ concentration data within the study region in 2016 were obtained from the China National Environmental Monitoring Center (CNEMC) website (http://www.cnemc.cn) and the Hubei Provincial Environmental Monitoring Center Station (HPEMCS) website (http://www.hbemc.com.cn/). In this study, 77 CNEMC stations and 27 HPEMCS stations (104 stations in total) were included. The distribution of the $PM_{2.5}$ monitoring stations is shown in Figure 1. It can be seen that the CNEMC stations are unevenly distributed, but the HPEMCS stations compensate for this. In light of the Chinese National Ambient Air Quality Standard, the ground-level $PM_{2.5}$ concentrations are usually measured with beta attenuation monitors (or beta-gauges) or by the tapered element oscillating microbalance method. Previous study indicated that they have an uncertainty of 0.75% for the hourly records (Engel-Cox et al., 2013). We averaged the hourly $PM_{2.5}$ to daily mean $PM_{2.5}$ data for the satellite-based estimation of $PM_{2.5}$. The reasons for not taking only the hourly measurements during the MODIS overpass time but using the daily mean $PM_{2.5}$ can be summarized as follows. First, the daily averages and yearly averages of $PM_{2.5}$ concentration have aroused more concern than hourly $PM_{2.5}$ data, and the interim targets were made based on the daily averages and yearly averages (Ministry of Ecology and Environment of the People's Republic of China, 2012; WHO, 2006). If the hourly $PM_{2.5}$ data are used, the satellite-based $PM_{2.5}$ retrievals can only reflect the $PM_{2.5}$ concentrations at some certain hours, then the daily averages and yearly averages are hard to obtain. Second, the integration of satellite remote sensing and ground stations is aimed at mapping the spatial distribution of $PM_{2.5}$. However, the satellite overpass time varies from location to location. If the hourly $PM_{2.5}$ data corresponding to the satellite overpass time are adopted, then the hourly $PM_{2.5}$ data at different times can be used in different places. Thus, the satellite-based $PM_{2.5}$ retrievals over a certain region can represent $PM_{2.5}$ concentrations at various times over different subregions. Finally, the daily mean $PM_{2.5}$ data have actually been extensively employed for satellite-based $PM_{2.5}$ estimation (Liu et al., 2005, 2007; Ma et al., 2016). For each monitoring station, the dates with less than 18-hourly observations were excluded from our analysis.

2.3. Satellite Observations

The Aqua MODIS Level 1B calibrated radiances (MYD02) product was downloaded from the Level 1 and Atmosphere Archive and Distribution System website (https://ladsweb.modaps.eosdis.nasa.gov). This product has a spatial resolution of 1 km at nadir. The TOA reflectance on bands 1, 3, and 7 (R1, R3, and R7) and observation angles (i.e., sensor azimuth, sensor zenith, solar azimuth, and solar zenith) are exploited for the retrieval of AOD via a dark-target-based algorithm (Kaufman, Tanré et al., 1997). The reflectance bands have wavelengths of 0.620–0.670, 0.459–0.479, and 2.105–2.155 μm, respectively. Despite the avoidance of AOD retrieval, these parameters were still extracted from the MYD02 product to estimate the ground-level $PM_{2.5}$. To eliminate the cloud contamination, the MODIS cloud mask product (MYD35_L2) was adopted, which is available at a resolution of 1 km every day. The cloud mask products have been reported to have a high accuracy when compared with the observations from ground-based and satellite-based LiDAR/radar (Ackerman et al., 2008). They have four confidence levels, that is, "cloudy," "uncertain clear," "probably clear," and "confident clear" (Ackerman et al., 1998). In this study, we only used the data with the highest confidence level (confident clear).

The MODIS normalized difference vegetation index (NDVI) product (Level 3, MYD13), with a resolution of 1 km every 16 days, was also downloaded from the Level 1 and Atmosphere Archive and Distribution System website. The MODIS NDVI was incorporated into the $PM_{2.5}$ estimation model to reflect the land-cover type. For comparison purposes, the MODIS AOD products of Collection 6 were utilized to establish the AOD-PM modeling. The data field of "Optical_Depth_Land_And_Ocean" was extracted in this study. These products have a spatial resolution of 3 km and are retrieved using a dark-target-based algorithm (Remer et al., 2013).

2.4. Meteorological Data

As the level of $PM_{2.5}$ concentration is associated with meteorological parameters (Yang et al., 2017), the Goddard Earth Observing System Data Assimilation System GEOS-5 Forward Processing (GEOS 5-FP; Lucchesi, 2013) meteorological data were incorporated in this study. GEOS 5-FP exploits an analysis developed jointly with NOAA's National Centers for Environmental Prediction, which allows the Global Modeling and Assimilation Office to take advantage of the developments at National Centers for

Environmental Prediction and the Joint Center for Satellite Data Assimilation. These GEOS 5-FP meteorological data have a spatial resolution of 0.25° latitude × 0.3125° longitude. Wind speed at 10 m above ground (WS, m/s), air temperature at a 2-m height (TMP, K), relative humidity (RH, %), surface pressure (PS, kPa), and planetary boundary layer height (PBL, m). If the abbreviations are excluded, readers will not understand the meaning of Equation (1) between 1 and 2 P.M. local time (the Aqua satellite overpass time corresponds to 1:30 P.M. local time) were used. More details can be found at the official website (https://fluid.nccs.nasa.gov/weather/).

2.5. Data Preprocessing and Matching

First, we created a 0.01° grid and a 0.03° grid for the Ref-PM modeling and the AOD-PM modeling, respectively. The data matching, model establishment, and spatial mapping were based on the established grids. For each grid, ground-level $PM_{2.5}$ measurements from multiple stations were averaged. Meanwhile, we resampled the meteorological data to match the satellite observations. All these data were reprojected to the same coordinate system. Finally, we extracted the satellite observations and meteorological parameters for the locations where $PM_{2.5}$ measurements were available.

3. Deep Learning Based Ref-PM Modeling for $PM_{2.5}$ Estimation

In the process of AOD retrieval, the satellite TOA reflectance bands and observation angles are utilized as the primary input in the atmospheric radiative transfer model. Although the Ref-PM modeling is aimed at avoiding the process of AOD retrieval and estimating ground-level $PM_{2.5}$ directly from satellite TOA reflectance, the original input (i.e., TOA reflectance and observation angles) is still adopted for the estimation of ground-level $PM_{2.5}$. The physical relationship between TOA reflectance and surface $PM_{2.5}$ is presented in supporting information Text S1 (Bilal et al., 2013; Gordon & Wang, 1994; Kaufman, Tanré et al., 1997; Kokhanovsky & Leeuw, 2009; Tanre et al., 1988; Vermote et al., 1997; Zhang & Li, 2015).

Generally, the structure of the Ref-PM modeling approach is depicted in equation (1). The dependent variable is $PM_{2.5}$ concentration, and the explanatory variables are satellite TOA reflectance (R1, R3, and R7), observation angles, meteorological parameters, and satellite NDVI. In addition, we incorporated the geographical correlation of $PM_{2.5}$ into the Ref-PM modeling approach, because the nearby $PM_{2.5}$ from the neighboring *s* grids and the $PM_{2.5}$ measurements from the prior *t* days for the same grid are useful information for the estimation of $PM_{2.5}$ (Di et al., 2016). In this study, *s*,*t* were set as 5 and 3 (Text S2), respectively.

$$PM_{2.5} = f(R1, R3, R7, angles, RH, WS, TMP, PBL, PS, NDVI, S\text{-}PM_{2.5}, T\text{-}PM_{2.5}, DIS), \quad (1)$$

where *f*() means the estimation function. *S* - $PM_{2.5}$, *T* - $PM_{2.5}$, *DIS* denote the geographical correlation of $PM_{2.5}$ (see our previous study for details of their calculation, T. Li, Shen, Yuan et al., 2017). *S* - $PM_{2.5}$ and *T* - $PM_{2.5}$ take the spatial and temporal autocorrelation of $PM_{2.5}$ into consideration, and *DIS* is incorporated to reflect the spatial heterogeneity of unevenly distributed stations. Instead of satellite-derived AOD, the satellite original signals (i.e., TOA reflectance and observation angles) are directly used to estimate ground-level $PM_{2.5}$. Thus, the key point of Ref-PM modeling is to mine the deep association between TOA reflectance and $PM_{2.5}$ via a statistic approach rather than a physical model.

The relationship between $PM_{2.5}$, satellite TOA reflectance, observation angles, and meteorological factors is very complex. Thus, deep learning, which has great potential for fitting nonlinear and complex relationships, was employed to represent the estimation function *f*(). In this study, a DBN (Hinton et al., 2006), which is one of the widely used deep learning models, was adopted for the estimation of ground-level $PM_{2.5}$. Figure 2 presents the structure of a DBN model containing two hidden layers. As illustrated in the figure, the basic unit is a restricted Boltzmann machine (RBM). An RBM contains a visible layer and a hidden layer, where the hidden layer of the prior RBM is the visible layer of the next RBM. The DBN consists of multiple RBMs and a back-propagation (BP) layer. This BP layer can be utilized for classification or prediction, and it is used here for the prediction of the ground-level $PM_{2.5}$. In this study, two RBM layers with 15 neurons in each RBM layer were chosen (Text S2). For details of the DBN model, we refer the readers to T. Li, Shen, Yuan et al. (2017). The procedure of this model for Ref-PM modeling is divided into three steps, which are shown in Figure 3.

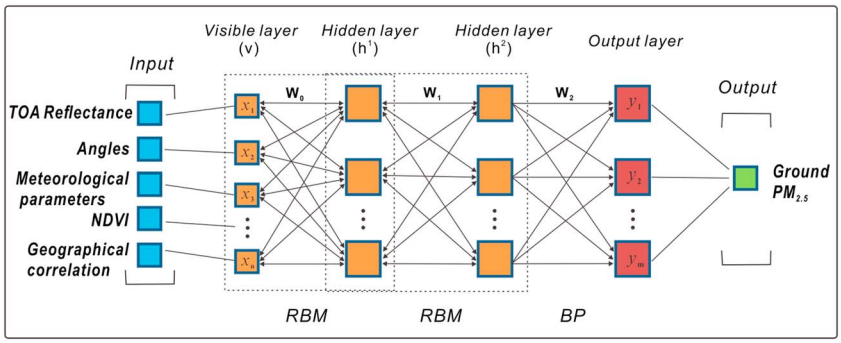

Figure 2. The structure of the deep belief network model for Ref-PM modeling. TOA = top-of-atmosphere; NDVI = normalized difference vegetation index; RBM = restricted Boltzmann machine; BP = back-propagation.

First, the satellite TOA reflectance, observation angles, meteorological parameters, NDVI, and geographical correlation of $PM_{2.5}$ are input into the DBN model. This model is pretrained using the input data themselves, and without the supervision of station measurements. In other words, the station $PM_{2.5}$ measurements are not used to tune the model coefficients in this step, and the initial model coefficients are trained from the input data.

Second, the estimated $PM_{2.5}$ can be obtained from the DBN model. Subsequently, we calculate the mean square error between the estimated $PM_{2.5}$ and ground-observed $PM_{2.5}$. The error is sent back to fine-tune the model coefficients using the BP algorithm (Rumelhart et al., 1986). This process is repeated until the model achieves a satisfactory performance. Through this step, the DBN model can effectively establish the relationship between $PM_{2.5}$ and satellite reflectance.

Finally, the model is validated and exploited to predict the $PM_{2.5}$ concentration on those locations with no ground monitoring stations. Thus, the distribution of $PM_{2.5}$ concentration can be acquired.

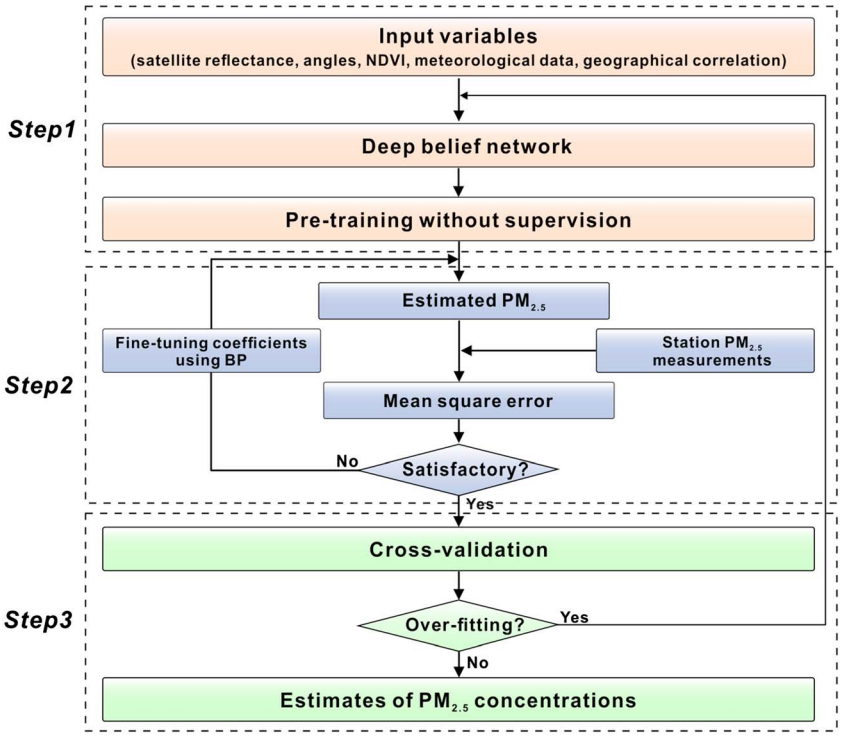

Figure 3. Flowchart describing the process of the deep belief network model for Ref-PM modeling. NDVI = normalized difference vegetation index; BP = back-propagation.

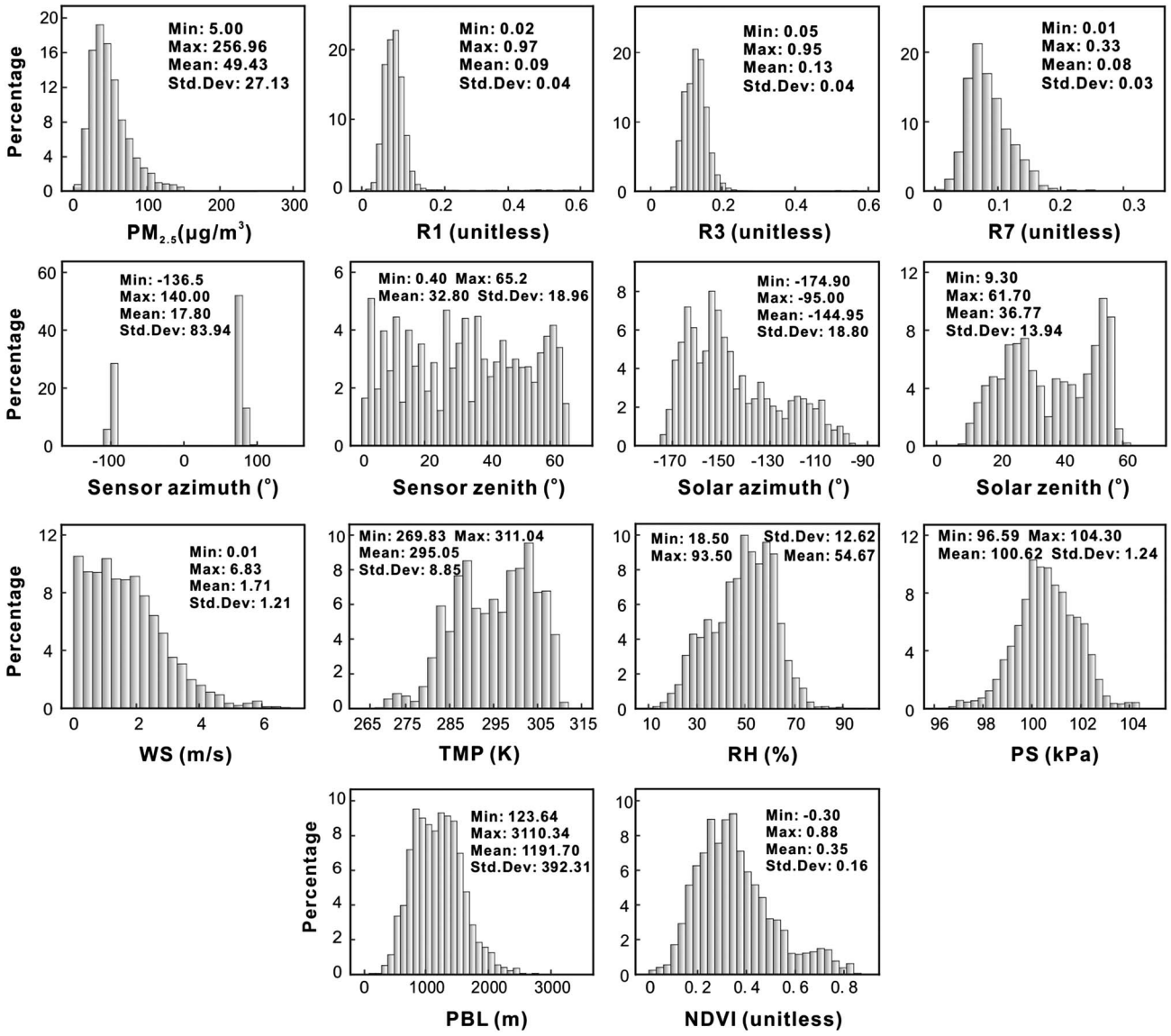

Figure 4. Histograms and descriptive statistics of the Ref-PM modeling variables in the sample data set. WS = wind speed; TMP = temperature; RH = relative humidity; PS = pressure; PBL = planetary boundary layer; NDVI = normalized difference vegetation index.

To evaluate the Ref-PM modeling, we compared it with the AOD-PM modeling. For the AOD-PM modeling, the inputs are satellite AOD, meteorological parameters, NDVI, and the geographical correlation of $PM_{2.5}$, and the specific model is the same as for the Ref-PM modeling, that is, the DBN model. Furthermore, we adopted a tenfold cross-validation (CV) technique (Rodriguez et al., 2010) to test the potential of model overfitting and the predictive power. Previous studies have usually used sample-based CV (T. Li, Shen, Zeng et al., 2017; Ma et al., 2014) or site-based CV (Lee et al., 2011a; Xie et al., 2015) to evaluate the model performance. In this study, both sample-based CV and site-based CV were chosen for the model validation. For the sample-based CV, all the samples in the model data set were randomly and equally divided into 10 subsets. One subset was used as the validation samples, and the other subsets were used to fit the model for each round of validation. For the site-based CV, we divided the monitoring stations into 10 subsets randomly and equally. One subset was used for the validation and the remaining stations were used for the model fitting in each round. We selected the statistical indicators of the coefficient of determination (R^2), the root-mean-square error (RMSE, $\mu g/m^3$), the mean prediction error ($\mu g/m^3$), and the relative prediction error (defined as RMSE divided by the mean ground-level $PM_{2.5}$) to give a quantitative evaluation of the model performance.

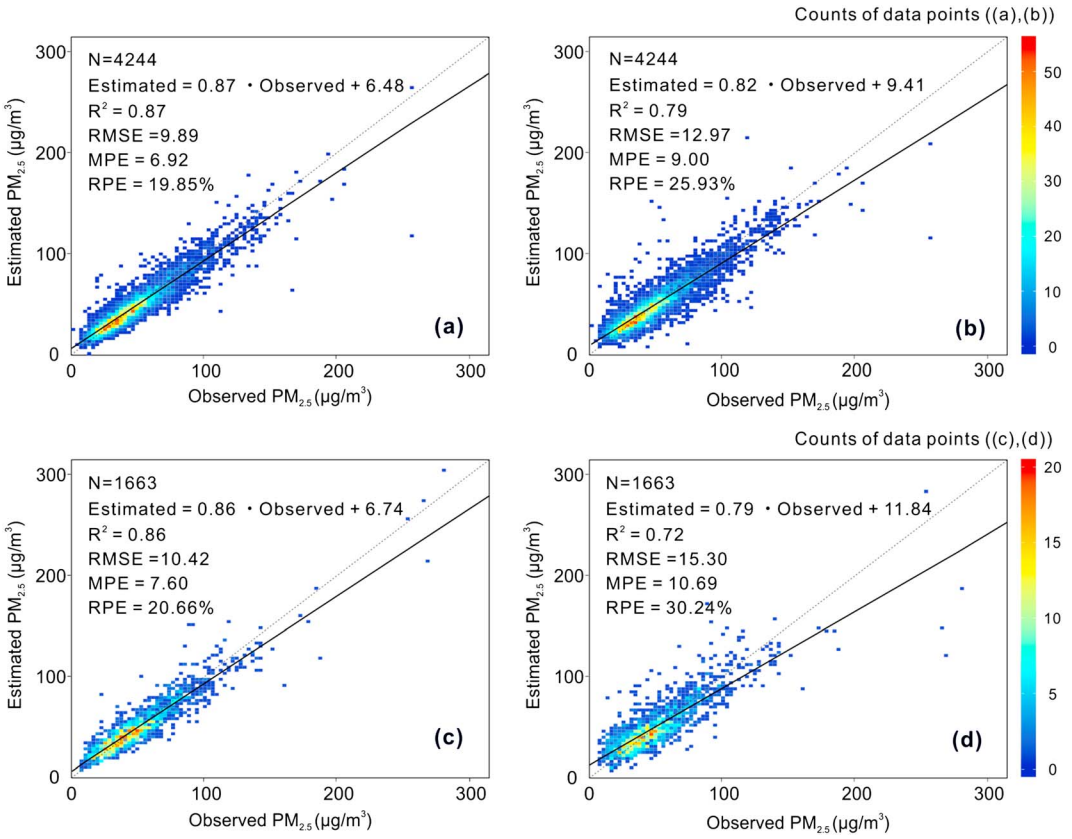

Figure 5. Scatter plots of the Ref-PM modeling and the AOD-PM modeling cross-validation results: (a) and (b) are the sample-based and site-based cross-validation results of the Ref-PM modeling; (c) and (d) are the sample-based and site-based cross-validation results of the AOD-PM modeling. RMSE = root-mean-square error; MPE = mean prediction error; RPE = relative prediction error.

4. Results and Discussion

4.1. Descriptive Statistics

Figure 4 presents the histograms and descriptive statistics of the variables in the sample data set. The $PM_{2.5}$ concentrations range from 5 μg/m^3 to 256.96 μg/m^3, with an average of 49.43 μg/m^3. R1, R3, and R7 are mostly distributed in the range of 0–0.2, with mean values of 0.09, 0.13, and 0.08, respectively. As a whole, the distributions of satellite TOA reflectance, relative humidity, surface pressure, height of planetary boundary layer, and NDVI appear similar with that of $PM_{2.5}$ concentration, while the other variables have different distribution patterns. The correlation coefficient between R1/R3/R7 and $PM_{2.5}$ is 0.10/0.12/−0.27, implying a nonlinear relationship between TOA reflectance and $PM_{2.5}$.

4.2. Performance of Ref-PM Modeling

Figure 5 shows the CV performance of Ref-PM modeling and AOD-PM modeling, respectively. The sample size of the AOD-PM modeling data set (N = 1663) is much smaller than that of the Ref-PM modeling data set (N = 4244). The main reason for this is that the TOA reflectance data have a finer spatial resolution and larger coverage than the AOD products. As can be observed from Figure 5, the Ref-PM modeling achieves an outstanding performance, with sample-based (site-based) CV R^2 and RMSE values of 0.87 (0.79) and 9.89 (12.97) μg/m^3, respectively. Meanwhile, the sample-based (site-based) CV R^2 and RMSE values of the AOD-PM modeling are 0.86 (0.72) and 10.42 (15.30) μg/m^3, respectively. It can be seen that the sample-based CV results of the Ref-PM modeling (R^2 = 0.87) show a slight advantage over the AOD-PM modeling (R^2 = 0.86). Meanwhile, the site-based CV results of the AOD-PM modeling report a larger decrease (from 0.79 to 0.72 for R^2) than the Ref-PM modeling. It is worth noting that the site-based CV approach, which uses a spatial hold-out validation strategy, can reflect the spatial predictive power more adequately (T. Li, Shen, Yuan et al.,

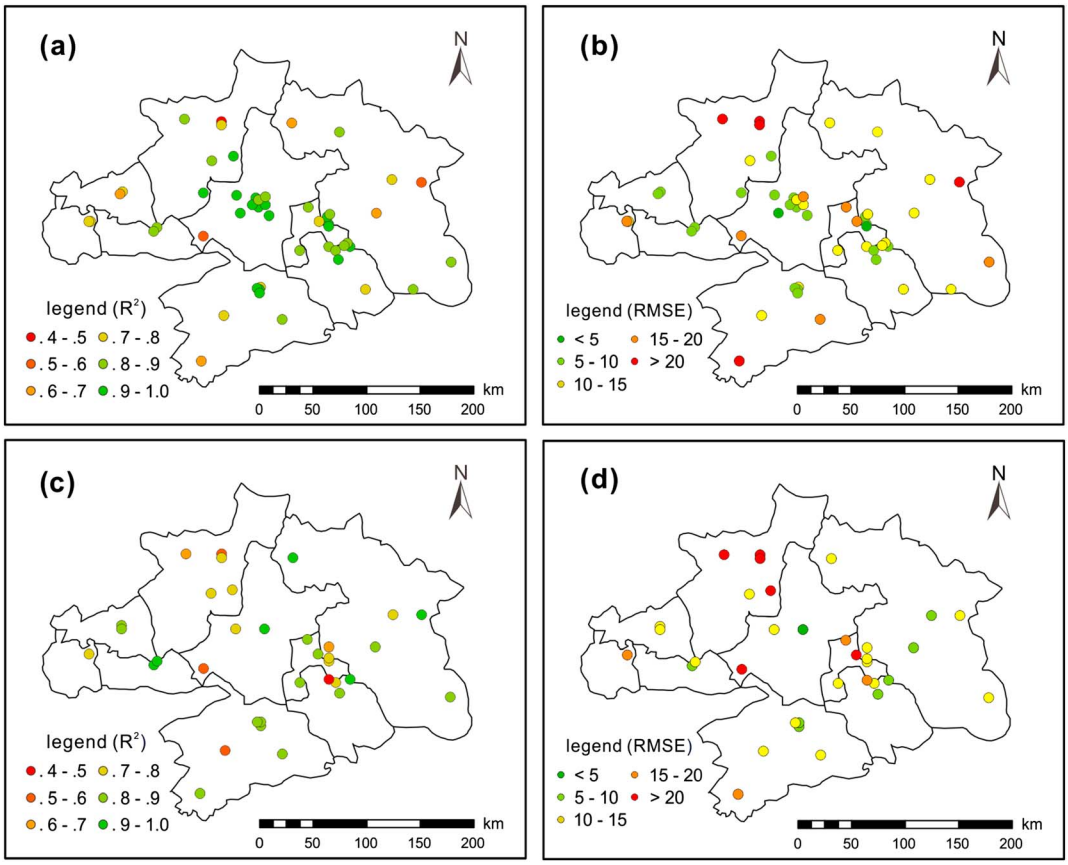

Figure 6. Spatial performance of the site-based cross-validation: (a) and (b) are, respectively, the R^2 and RMSE values for the Ref-PM modeling; (c) and (d) are, respectively, the R^2 and RMSE values for the AOD-PM modeling. RMSE = root-mean-square error.

2017). Hence, the results indicate that the Ref-PM modeling approach has a superior spatial predictive power than AOD-PM modeling.

Another finding worth noting in Figure 5 is that the sample-based and site-based CV slopes for the Ref-PM modeling are 0.87 and 0.82, respectively. This means that the proposed Ref-PM modeling approach tends to underestimate when the ground-level $PM_{2.5}$ concentrations are greater than ~50 μg/m^3. Meanwhile, the AOD-PM modeling reports a slightly higher extent of underestimation, with sample-based and site-based CV slopes of 0.86 and 0.79, respectively. The possible reason for this underestimation could be that we exploited a spatially averaged modeling framework and point-based monitoring data. For a given grid, a great estimation of the spatially averaged concentration may not be given by the sampling distribution of the monitoring stations (T. Li, Shen, Yuan et al., 2017). Another possible reason is the lack of samples in the training data set with higher $PM_{2.5}$ values. It is difficult for the model to capture the features of higher $PM_{2.5}$ concentrations, and thus the model tends to underestimate high values.

The spatial site-based CV performance of the Ref-PM modeling and the AOD-PM modeling was also evaluated. The R^2 and RMSE values between the observed $PM_{2.5}$ and estimated $PM_{2.5}$ on each grid were calculated (see Table S1), and are shown in Figure 6. Overall, the Ref-PM modeling approach achieves a satisfactory performance, with 70% of the grids reporting a high R^2 value of greater than 0.80, and low RMSE values ($<$15 μg/m^3) are found on 81% of the grids. For the AOD-PM modeling, only 58% of the grids have R^2 values of greater than 0.80, and the grids with RMSE values of less than 15 μg/m^3 account for 73%. These statistics indicate that the Ref-PM modeling approach shows some superiorities in the spatial prediction of $PM_{2.5}$ over AOD-PM modeling. Some spatial variations can also be observed in Figure 6. For instance, compared with the results of the AOD-PM modeling, some advantages are found in Wuhan for the Ref-PM modeling. In contrast, the AOD-PM modeling achieves a slightly better result than the Ref-PM modeling in the regions of Huanggang.

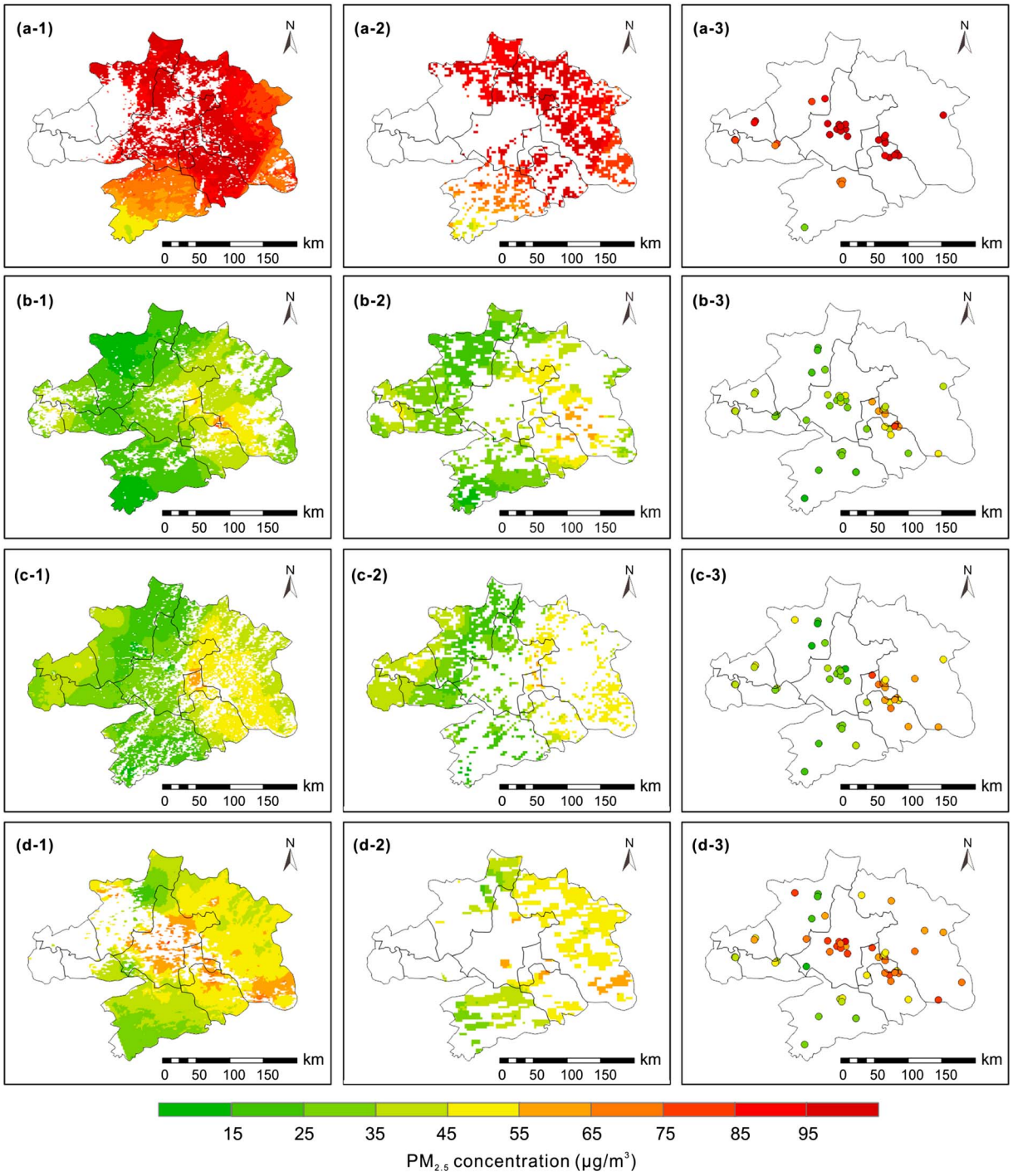

Figure 7. Daily estimates of $PM_{2.5}$ on some specific days (1 day in each season, and these days have as much as valid data). From top to bottom: (a) 20160115, (b) 20160516, (c) 20160725, and (d) 20161127. Left column: top-of-atmosphere reflectance based estimation of $PM_{2.5}$. Middle column: aerosol optical depth-based estimation of $PM_{2.5}$. Right column: ground station measurements. The white regions indicate missing data.

4.3. Discussion

The retrieval of AOD often meets a challenge, which is the bright surfaces (e.g., R7 > 0.15, C. Li et al., 2005). The 3-km AOD products used here are retrieved via dark-target-based algorithms, and have no retrievals on bright surface regions. Thus, the AOD-based estimation of $PM_{2.5}$ is often missing on these regions. In this study, the TOA reflectance on bright surfaces was included to estimate ground-level

$PM_{2.5}$. As illustrated in Figure 7, the reflectance-derived $PM_{2.5}$ has a larger spatial coverage than the AOD- derived $PM_{2.5}$, which can largely be attributed to the estimates on bright surfaces. We evaluated the performance of the Ref-PM modeling approach on the bright surfaces. The results show that the sample-based cross-validated R^2 value is 0.80 on the bright surface regions and 0.87 on the dark target regions. It can therefore be concluded that the accuracy of the $PM_{2.5}$ estimation on bright surfaces is acceptable, and Ref-PM modeling can effectively estimate ground-level $PM_{2.5}$ on bright surface regions. It can also be observed in Figure 7 that the reflectance-derived $PM_{2.5}$ has a finer resolution than the AOD-derived $PM_{2.5}$. Owing to the larger coverage and finer resolution, the reflectance-derived $PM_{2.5}$ has the capacity to provide more details for pollution monitoring.

In this study, we selected R1, R3, R7, and observation angles from MODIS observations for the model development. The physical explanations for the selection can be summarized as follows. First, the reflectance of most land surfaces is relatively low in blue channel, and the atmosphere may make a larger contribution to TOA reflectance. The aerosol appears to be separated from the TOA reflectance more easily. For the red channel, it also reports relatively low surface reflectance on dark targets (e.g., vegetation), and there is little absorption of dust (Hsu et al., 2004). Hence, R1 (red channel) and R3 (blue channel) from MODIS have been widely used for aerosol retrieval (Kaufman, Tanré et al., 1997; Levy et al., 2007). Second, the 2.1 μm band (band 7) is only slightly influenced by the atmosphere compared to the visible bands, and R7 is often adopted for the recognition of surface types (e.g., dark targets), and to obtain the surface reflectance (Kaufman, Wald et al., 1997). Furthermore, the observation angles were employed because they are important parameters in the physical relationship between TOA reflectance and surface $PM_{2.5}$, which is presented in Text S1.

This study provides an effective solution for the estimation of ground-level $PM_{2.5}$ from satellite TOA reflectance rather than AOD products. However, the satellite-derived AOD is still one of the most important atmospheric parameters. For example, the AOD data are an indicator of atmospheric pollution and play an important role in research on aerosol-cloud interaction, climate change, and so forth. This paper only suggests that for the estimation of ground-level $PM_{2.5}$, it appears possible to avoid the retrieval of satellite AOD. The proposed solution could also be extended to the monitoring of other environmental features (Lary et al., 2016, 2018), especially when no proper satellite parameters such as AOD are available. Therefore, this study has no intention to belittle satellite AOD retrieval or AOD-PM modeling, but instead proposes a new solution for the satellite-based estimation of ground-level $PM_{2.5}$.

5. Conclusions and Future Work

In this paper, the Ref-PM modeling approach was developed to avoid the intermediate process of AOD retrieval and to estimate ground-level $PM_{2.5}$ directly from satellite TOA reflectance without a physical model. Using the WUA as an example, the results show that, compared with AOD-PM modeling, the Ref-PM modeling approach achieves a competitive performance, with sample-based CV R^2 and RMSE values of 0.87 and 9.89 $\mu g/m^3$, respectively. The daily distribution of $PM_{2.5}$ in the WUA was also mapped, and the reflectance-derived $PM_{2.5}$ has a finer resolution and larger spatial coverage than the AOD-derived $PM_{2.5}$. All these results indicate that the proposed Ref-PM modeling approach has the capacity to estimate ground-level $PM_{2.5}$ concentration directly from satellite TOA reflectance. This study provides an alternative technique to estimate ground-level $PM_{2.5}$, and will provide useful information for pollution monitoring and control.

Our future studies will focus on two aspects. First, the Ref-PM modeling approach has achieved some reasonable results for the estimation of $PM_{2.5}$ directly from TOA reflectance. However, we only selected R1, R3, R7, and observation angles for the model establishment. Would the incorporation of surface reflectance data (e.g., MOD09) boost the accuracy of $PM_{2.5}$ estimation? Whether or not more/other satellite parameters can better explain $PM_{2.5}$ concentration still has room for exploration. Second, the proposed Ref-PM modeling approach was validated in the small region of the WUA. Larger geographic regions may bring new challenges and problems. The application and validation of the Ref-PM modeling approach in large geographic regions will be conducted in our future studies.

Acknowledgments

This work was funded by the National Key R&D Program of China (2016YFC0200900) and the National Natural Science Foundation of China (41422108). The ground-level $PM_{2.5}$ data are provided by the China National Environmental Monitoring Center (http://www.cnemc.cn) and the Hubei Provincial Environmental Monitoring Center Station (http://www.hbemc.com.cn/). The meteorological data are available from the Goddard Space Flight Center (https://fluid.nccs.nasa.gov/weather/). The satellite data are available from the Level-1 and Atmosphere Archive & Distribution System (https://ladsweb.modaps.eosdis.nasa.gov). The data used are listed in section 2.

References

Ackerman, S. A., Holz, R. E., Frey, R., Eloranta, E. W., Maddux, B. C., & McGill, M. (2008). Cloud detection with MODIS. Part II: Validation. *Journal of Atmospheric and Oceanic Technology*, *25*(7), 1073–1086. https://doi.org/10.1175/2007JTECHA1053.1

Ackerman, S. A., Strabala, K. I., Menzel, W. P., Frey, R. A., Moeller, C. C., & Gumley, L. E. (1998). Discriminating clear sky from clouds with MODIS. *Journal of Geophysical Research*, *103*(D24), 32,141–32,157. https://doi.org/10.1029/1998JD200032

Bilal, M., Nichol, J. E., Bleiweiss, M. P., & Dubois, D. (2013). A simplified high resolution MODIS aerosol retrieval algorithm (SARA) for use over mixed surfaces. *Remote Sensing of Environment*, *136*, 135–145. https://doi.org/10.1016/j.rse.2013.04.014

Brauer, M., Amann, M., Burnett, R. T., Cohen, A., Dentener, F., Ezzati, M., et al. (2012). Exposure assessment for estimation of the global burden of disease attributable to outdoor air pollution. *Environmental Science & Technology*, *46*(2), 652–660. https://doi.org/10.1021/es2025752

Crouse, D. L., Peters, P. A., van Donkelaar, A., Goldberg, M. S., Villeneuve, P. J., Brion, O., et al. (2012). Risk of nonaccidental and cardiovascular mortality in relation to long-term exposure to low concentrations of fine particulate matter: A Canadian national-level cohort study. *Environmental Health Perspectives*, *120*(5), 708–714. https://doi.org/10.1289/ehp.1104049

Di, Q., Koutrakis, P., & Schwartz, J. (2016). A hybrid prediction model for PM2.5 mass and components using a chemical transport model and land use regression. *Atmospheric Environment*, *131*, 390–399. https://doi.org/10.1016/j.atmosenv.2016.02.002

Engel-Cox, J., Kim Oanh, N. T., van Donkelaar, A., Martin, R. V., & Zell, E. (2013). Toward the next generation of air quality monitoring: Particulate matter. *Atmospheric Environment*, *80*, 584–590. https://doi.org/10.1016/j.atmosenv.2013.08.016

Fang, X., Zou, B., Liu, X., Sternberg, T., & Zhai, L. (2016). Satellite-based ground PM2.5 estimation using timely structure adaptive modeling. *Remote Sensing of Environment*, *186*, 152–163. https://doi.org/10.1016/j.rse.2016.08.027

Gordon, H. R., & Wang, M. (1994). Retrieval of water-leaving radiance and aerosol optical thickness over the oceans with SeaWiFS: A preliminary algorithm. *Applied Optics*, *33*(3), 443–452. https://doi.org/10.1364/AO.33.000443

Gupta, P., & Christopher, S. A. (2009a). Particulate matter air quality assessment using integrated surface, satellite, and meteorological products: 2. A neural network approach. *Journal of Geophysical Research*, *114*, D20205. https://doi.org/10.1029/2008JD011497

Gupta, P., & Christopher, S. A. (2009b). Particulate matter air quality assessment using integrated surface, satellite, and meteorological products: Multiple regression approach. *Journal of Geophysical Research*, *114*, D14205. https://doi.org/10.1029/2008JD011496

Habre, R., Moshier, E., Castro, W., Nath, A., Grunin, A., Rohr, A., et al. (2014). The effects of PM2.5 and its components from indoor and outdoor sources on cough and wheeze symptoms in asthmatic children. *Journal of Exposure Science & Environmental Epidemiology*, *24*(4), 380–387. https://doi.org/10.1038/jes.2014.21

Hinton, G. E., Osindero, S., & Teh, Y.-W. (2006). A fast learning algorithm for deep belief nets. *Neural Computation*, *18*(7), 1527–1554. https://doi.org/10.1162/neco.2006.18.7.1527

Hoff, R. M., & Christopher, S. A. (2009). Remote sensing of particulate pollution from space: Have we reached the promised land? *Journal of the Air & Waste Management Association*, *59*(6), 645–675. https://doi.org/10.3155/1047-3289.59.6.645

Hsu, N. C., Tsay, S.-C., King, M. D., & Herman, J. R. (2004). Aerosol properties over bright-reflecting source regions. *IEEE Transactions on Geoscience and Remote Sensing*, *42*(3), 557–569. https://doi.org/10.1109/TGRS.2004.824067

Hu, X., Waller, L. A., Al-Hamdan, M. Z., Crosson, W. L., Estes, M. G. Jr., Estes, S. M., et al. (2013). Estimating ground-level PM2.5 concentrations in the southeastern U.S. using geographically weighted regression. *Environmental Research*, *121*, 1–10. https://doi.org/10.1016/j.envres.2012.11.003

Kaufman, Y. J., Tanré, D., Remer, L. A., Vermote, E. F., Chu, A., & Holben, B. N. (1997). Operational remote sensing of tropospheric aerosol over land from EOS moderate resolution imaging spectroradiometer. *Journal of Geophysical Research*, *102*(D14), 17,051–17,067. https://doi.org/10.1029/96JD03988

Kaufman, Y. J., Wald, A. E., Remer, L. A., Bo-Cai, G., Rong-Rong, L., & Flynn, L. (1997). The MODIS 2.1-μm channel-correlation with visible reflectance for use in remote sensing of aerosol. *IEEE Transactions on Geoscience and Remote Sensing*, *35*(5), 1286–1298. https://doi.org/10.1109/36.628795

Kokhanovsky, A., & Leeuw, G. D. (2009). *Satellite aerosol remote sensing over land*. Springer. https://doi.org/10.1007/978-3-540-69397-0

Lary, D. J., Alavi, A. H., Gandomi, A. H., & Walker, A. L. (2016). Machine learning in geosciences and remote sensing. *Geoscience Frontiers*, *7*(1), 3–10. https://doi.org/10.1016/j.gsf.2015.07.003

Lary, D. J., Faruque, F. S., Malakar, N., Moore, A., Roscoe, B., Adams, Z. L., & Eggelston, Y. (2014). Estimating the global abundance of ground level presence of particulate matter (PM2.5). *Geospatial Health*, *8*(3), 611–S630. https://doi.org/10.4081/gh.2014.292

Lary, D. J., Lary, T., & Sattler, B. (2015). Using machine learning to estimate global PM2.5 for environmental health studies. *Environmental Health Insights*, *9s1*, EHI.S15664. https://doi.org/10.4137/EHI.S15664

Lary, D. J., Zewdie, G. K., Liu, X., Wu, D., Levetin, E., Allee, R. J., et al. (2018). Machine learning applications for Earth observation. In P.-P. Mathieu, & C. Aubrecht (Eds.), *Earth observation open science and innovation* (pp. 165–218). Cham: Springer International Publishing. https://doi.org/10.1007/978-3-319-65633-5_8

LeCun, Y., Bengio, Y., & Hinton, G. (2015). Deep learning. *Nature*, *521*(7553), 436–444. https://doi.org/10.1038/nature14539

Lee, H., Liu, Y., Coull, B., Schwartz, J., & Koutrakis, P. (2011a). A novel calibration approach of MODIS AOD data to predict PM2. 5 concentrations. *Atmospheric Chemistry and Physics*, *11*(15), 7991–8002. https://doi.org/10.5194/acp-11-7991-2011

Lee, H. J., Liu, Y., Coull, B., Schwartz, J., & Koutrakis, P. (2011b). PM2.5 prediction modeling using MODIS AOD and its implications for health effect studies. *Epidemiology*, *22*(1), S215.

Levy, R. C., Remer, L. A., Mattoo, S., Vermote, E. F., & Kaufman, Y. J. (2007). Second-generation operational algorithm: Retrieval of aerosol properties over land from inversion of Moderate Resolution Imaging Spectroradiometer spectral reflectance. *Journal of Geophysical Research*, *112*, D13211. https://doi.org/10.1029/2006JD007811

Li, C., Lau, A. K. H., Mao, J., & Chu, D. A. (2005). Retrieval, validation, and application of the 1-km aerosol optical depth from MODIS measurements over Hong Kong. *IEEE Transactions on Geoscience and Remote Sensing*, *43*(11), 2650–2658. https://doi.org/10.1109/TGRS.2005.856627

Li, T., Shen, H., Yuan, Q., Zhang, X., & Zhang, L. (2017). Estimating ground-level PM2.5 by fusing satellite and station observations: A geo-intelligent deep learning approach. *Geophysical Research Letters*, *44*, 11,985–911,993. https://doi.org/10.1002/2017GL075710

Li, T., Shen, H., Zeng, C., Yuan, Q., & Zhang, L. (2017). Point-surface fusion of station measurements and satellite observations for mapping PM2.5 distribution in China: Methods and assessment. *Atmospheric Environment*, *152*, 477–489. https://doi.org/10.1016/j.atmosenv.2017.01.004

Li, Z., Zhang, Y., Shao, J., Li, B., Hong, J., Liu, D., Li, D., et al. (2016). Remote sensing of atmospheric particulate mass of dry PM2.5 near the ground: Method validation using ground-based measurements. *Remote Sensing of Environment*, *173*, 59–68. https://doi.org/10.1016/j.rse.2015.11.019

Lim, S. S., Vos, T., Flaxman, A. D., Danaei, G., Shibuya, K., Adair-Rohani, H., et al. (2012). A comparative risk assessment of burden of disease and injury attributable to 67 risk factors and risk factor clusters in 21 regions, 1990–2010: A systematic analysis for the global burden of disease study 2010. *The Lancet*, *380*(9859), 2224–2260. https://doi.org/10.1016/S0140-6736(12)61766-8

Liu, Y., Franklin, M., Kahn, R., & Koutrakis, P. (2007). Using aerosol optical thickness to predict ground-level PM2.5 concentrations in the St. Louis area: A comparison between MISR and MODIS. *Remote Sensing of Environment*, *107*(1–2), 33–44. https://doi.org/10.1016/j.rse.2006.05.022

Liu, Y., Paciorek, C. J., & Koutrakis, P. (2009). Estimating regional spatial and temporal variability of PM(2.5) concentrations using satellite data, meteorology, and land use information. *Environmental Health Perspectives*, *117*(6), 886–892. https://doi.org/10.1289/ehp.0800123

Liu, Y., Sarnat, J. A., Kilaru, V., Jacob, D. J., & Koutrakis, P. (2005). Estimating ground-level PM2.5 in the eastern United States using satellite remote sensing. *Environmental Science & Technology*, *39*(9), 3269–3278. https://doi.org/10.1021/es049352m

Lucchesi, R. (2013). File specification for GEOS-5 FP. GMAO Office Note No. 4 (Version 1.0).

Ma, Z., Hu, X., Huang, L., Bi, J., & Liu, Y. (2014). Estimating ground-level PM2.5 in China using satellite remote sensing. *Environmental Science & Technology*, *48*(13), 7436–7444. https://doi.org/10.1021/es5009399

Ma, Z., Hu, X., Sayer, A. M., Levy, R., Zhang, Q., Xue, Y., et al. (2016). Satellite-based spatiotemporal trends in PM2.5 concentrations: China, 2004–2013. *Environmental Health Perspectives*, *124*(2), 184–192. https://doi.org/10.1289/ehp.1409481

Madrigano, J., Kloog, I., Goldberg, R., Coull, B. A., Mittleman, M. A., & Schwartz, J. (2013). Long-term exposure to PM(2.5) and incidence of acute myocardial infarction. *Environmental Health Perspectives*, *121*(2), 192–196. https://doi.org/10.1289/ehp.1205284

Martin, R. V. (2008). Satellite remote sensing of surface air quality. *Atmospheric Environment*, *42*(34), 7823–7843. https://doi.org/10.1016/j.atmosenv.2008.07.018

Ministry of Ecology and Environment of the People's Republic of China. (2012). Ambient air quality standards (GB3095–2012). http://kjs.mep.gov.cn/hjbhbz/bzwb/dqhjbh/dqhjzlbz/201203/t20120302_224165.htm

Munchak, L. A., Levy, R. C., Mattoo, S., Remer, L. A., Holben, B. N., Schafer, J. S., et al. (2013). MODIS 3 km aerosol product: Applications over land in an urban/suburban region. *Atmospheric Measurement Techniques*, *6*(7), 1747–1759. https://doi.org/10.5194/amt-6-1747-2013

Ong, B. T., Sugiura, K., & Zettsu, K. (2015). Dynamically pre-trained deep recurrent neural networks using environmental monitoring data for predicting PM2.5. *Neural Computing and Applications*, 1–14.

Paciorek, C. J., Liu, Y., Moreno-Macias, H., & Kondragunta, S. (2008). Spatiotemporal associations between GOES aerosol optical depth retrievals and ground-level PM2.5. *Environmental Science & Technology*, *42*(15), 5800–5806. https://doi.org/10.1021/es703181j

Radosavljevic, V., Vucetic, S., & Obradovic, Z. (2007). Aerosol optical depth retrieval by neural networks ensemble with adaptive cost function. Paper presented at the the 10th International Conference on Engineering Applications of Neural Networks.

Remer, L. A., Mattoo, S., Levy, R. C., & Munchak, L. A. (2013). MODIS 3 km aerosol product: Algorithm and global perspective. *Atmospheric Measurement Techniques*, *6*(7), 1829–1844. https://doi.org/10.5194/amt-6-1829-2013

Ristovski, K., Vucetic, S., & Obradovic, Z. (2012). Uncertainty analysis of neural-network-based aerosol retrieval. *IEEE Transactions on Geoscience and Remote Sensing*, *50*(2), 409–414. https://doi.org/10.1109/TGRS.2011.2166120

Rodriguez, J. D., Perez, A., & Lozano, J. A. (2010). Sensitivity analysis of k-fold cross validation in prediction error estimation. *IEEE Transactions on Pattern Analysis and Machine Intelligence*, *32*(3), 569–575. https://doi.org/10.1109/TPAMI.2009.187

Rumelhart, D. E., Hinton, G. E., & Williams, R. J. (1986). Learning representations by back-propagating errors. *Nature*, *323*(6088), 533–536. https://doi.org/10.1038/323533a0

Tan, R., Liu, Y., Liu, Y., He, Q., Ming, L., & Tang, S. (2014). Urban growth and its determinants across the Wuhan urban agglomeration, Central China. *Habitat International*, *44*, 268–281. https://doi.org/10.1016/j.habitatint.2014.07.005

Tanre, D., Deschamps, P. Y., Devaux, C., & Herman, M. (1988). Estimation of Saharan aerosol optical thickness from blurring effects in thematic mapper data. *Journal of Geophysical Research*, *93*(D12), 15,955–15,964. https://doi.org/10.1029/JD093iD12p15955

van Donkelaar, A., Martin, R. V., Brauer, M., Hsu, N. C., Kahn, R. A., Levy, R. C., et al. (2016). Global estimates of fine particulate matter using a combined geophysical-statistical method with information from satellites, models, and Monitors. *Environmental Science & Technology*, *50*(7), 3762–3772. https://doi.org/10.1021/acs.est.5b05833

Vermote, E. F., Tanre, D., Deuze, J. L., Herman, M., & Morcette, J. J. (1997). Second simulation of the satellite signal in the solar Spectrum, 6S: An overview. *IEEE Transactions on Geoscience and Remote Sensing*, *35*(3), 675–686. https://doi.org/10.1109/36.581987

Wang, L., Gong, W., Li, J., Ma, Y., & Hu, B. (2014). Empirical studies of cloud effects on ultraviolet radiation in Central China. *International Journal of Climatology*, *34*(7), 2218–2228. https://doi.org/10.1002/joc.3832

Wang, L., Gong, W., Xia, X., Zhu, J., Li, J., & Zhu, Z. (2015). Long-term observations of aerosol optical properties at Wuhan, an urban site in Central China. *Atmospheric Environment*, *101*, 94–102. https://doi.org/10.1016/j.atmosenv.2014.11.021

WHO (2006). *Air quality guidelines: Global update 2005: Particulate matter, ozone, nitrogen dioxide, and sulfur dioxide*. Copenhagen: World Health Organization.

Wu, J., Yao, F., Li, W., & Si, M. (2016). VIIRS-based remote sensing estimation of ground-level PM2.5 concentrations in Beijing–Tianjin–Hebei: A spatiotemporal statistical model. *Remote Sensing of Environment*, *184*, 316–328. https://doi.org/10.1016/j.rse.2016.07.015

Xie, Y., Wang, Y., Zhang, K., Dong, W., Lv, B., & Bai, Y. (2015). Daily estimation of ground-level PM2.5 concentrations over Beijing using 3 km resolution MODIS AOD. *Environmental Science & Technology*, *49*(20), 12,280–12,288. https://doi.org/10.1021/acs.est.5b01413

Yang, Q., Yuan, Q., Li, T., Shen, H., & Zhang, L. (2017). The relationships between PM2.5 and meteorological factors in China: Seasonal and regional variations. *International Journal of Environmental Research and Public Health*, *14*(12), 1510. https://doi.org/10.3390/ijerph14121510

You, W., Zang, Z., Pan, X., Zhang, L., & Chen, D. (2015). Estimating PM2.5 in Xi'an, China using aerosol optical depth: A comparison between the MODIS and MISR retrieval models. *Science of the Total Environment*, *505*, 1156–1165. https://doi.org/10.1016/j.scitotenv.2014.11.024

Zhang, Y., & Li, Z. (2015). Remote sensing of atmospheric fine particulate matter (PM2.5) mass concentration near the ground from satellite observation. *Remote Sensing of Environment*, *160*, 252–262. https://doi.org/10.1016/j.rse.2015.02.005

Zheng, C., Zhao, C., Zhu, Y., Wang, Y., Shi, X., Wu, X., et al. (2017). Analysis of influential factors for the relationship between PM2. 5 and AOD in Beijing. *Atmospheric Chemistry and Physics*, *17*(21), 13,473–13,489. https://doi.org/10.5194/acp-17-13473-2017